Silicon (2018) 10:1291–1303
https://doi.org/10.1007/s12633-017-9604-3

ORIGINAL PAPER

Investigation of the Thermal and Dielectric Behavior of Epoxy Nano-Hybrids by using Silane Modified Nano-ZnO

S. Suresh[1,2] · P. Nisha[3] · P. Saravanan[4] · K. Jayamoorthy[4] · S. Karthikeyan[5]

Received: 23 May 2016 / Accepted: 30 June 2017 / Published online: 24 October 2017

Abstract The present work focuses on a comparative study of the thermal and electrical behavior of diglycidyl ethers of bisphenol-A (DGEBA) to uncover the suitability for its use in high performance applications. An epoxy nanohybrids coating was developed using aminosilane functionalized ZnO (1, 3, 5 and 7 wt%) as the dispersed phase and commercially available DGEBA as the matrix phase, with curing using triethylenetetramine (TETA). The structural features of these materials were ascertained by FTIR spectral studies, SEM and AFM analyses. The peak shift in all the samples at $\sim$ 1032 cm^{-1} explains the etheric linkage of ZnO-APTES core shell nanoparticles with the DGEBA virgin epoxy resin. The thermal behavior of the diglycidyl resins and their corresponding nano-hybrids was studied by TGA and DSC. The first decomposition stage of DGEBA neat epoxy resin starts at 325 °C and the second stage at 513.2 °C which varied in all epoxy nanocomposites. Further thermodynamic parameters are calculated using the Coats-Redfern method from TGA results to examine the thermal stability. The sample with 3% ZnO-APTES-DGEBA film exhibits the highest activation energy of 26.20 kj/mol. The dielectric permittivity, dielectric loss and AC conductivity variation with frequency, temperature and filler concentration were studied using an impedance analyzer. The variation in electrical behavior is more pronounced in 1 and 7% ZnO-APTES-DGEBA epoxy nanocomposites.

Keywords Composite materials · Polymers · Silane · Dielectric · Epoxy resin

Electronic supplementary material The online version of this article (https://doi.org/10.1007/s12633-017-9604-3) contains supplementary material, which is available to authorized users.

✉ S. Suresh
profsuresh1@gmail.com

[1] Department of Physics, St. Joseph's College of Engineering, Chennai 600119, Tamilnadu, India

[2] Department of Research and Development Centre, Bharathiar University, Coimbatore 641046, Tamilnadu, India

[3] Department of Electrical and Electronics Engineering, Jeppiaar Engineering College, Chennai 600119, Tamilnadu, India

[4] Department of Chemistry, St. Joseph's College of Engineering, Chennai 600119, Tamilnadu, India

[5] Department of Physics, Dr. Ambedkar Government Arts College, Chennai 600039, Tamilnadu, India

1 Introduction

Nanotechnology has created a key revolution in the twenty first century exploiting the new properties, phenomena and functionalities exhibited by matter when dealt with at the level of a few nanometers. At this level, the physical, chemical and biological properties of materials differ in fundamental and valuable ways from properties of individual atoms and molecules or bulk matter. Research and development in nanotechnology is directed towards understanding and creating new materials, devices and systems that exploit these new properties [1]. In the last decade many research teams from all over the world have focused their energies toward studies on polymer nanocomposites as effective materials for electrical insulation [2]. These materials, also called nanodielectrics, are usually made of polymers

uniformly filled, from 1 to 10 wt%, with particles with at least one dimension from 1 to 100 nm. The increasing interest in the behavior of these new dielectrics is mainly due to the fact that these materials possess a huge filler-polymer matrix interface which has a major influence on the electrical, thermal and mechanical properties [3]. In order to improve the performance of organic polymers, different combinations of (mainly inorganic) nanofillers have been added and actively examined. Polymers such as polyamide (PA), polyethylene (PE), polypropylene (PP), ethylene vinyl acetate (EVA), epoxy resins and silicone rubbers were combined with nanofillers such as layered silicates (LS), silica (SiO_2), titania (TiO_2), Zinc (ZnO) and alumina (Al_2O_3) for improved performance [4]. The properties of nanocomposites certainly depend on the kind of nanoparticle materials, physical and chemical conditions of their surfaces, the kind of coupling agents to bridge inorganic and organic substances chemically and physically, the kind and content of compatibilizers and/or dispersants and the kind of polymer matrices [5]. Epoxy resins were chosen for our current studies as they have several excellent properties such as excellent toughness, adhesion and chemical resistance [6–8]. However, they do not possess adequate thermal and mechanical properties to meet the requirements of high-performance structural products. Hence, modification of epoxy resins using suitable modifiers such as silicone, polyhedral oligomeric silsesquioxanes (POSS) and nanoclay is mandatory. Demands for epoxy resins are extremely high because of their wide application as adhesives, coatings and as advanced composites in aerospace and electronics industries [9]. Incorporation of silane modified nanoparticles into the epoxy resin makes the resin become transparent, helps the resin withstand exposure to water, chemicals, increases the resistance of the resin to thermal oxidation and leads to easy processing [10]. In this work, we report our preliminary results obtained on electrical and thermal behavior of DGBEA and epoxy nanocomposites dispersed with APTES-ZnO. The electrical properties were studied with dielectric spectroscopy whereas thermal properties were studied with TG-DTA and DSC. The dielectric permittivity, dielectric loss and the AC conductivity were analyzed over a frequency range of 1 Hz–1 MHz and at various temperatures of 40 °C, 80 °C and 120 °C. The influence of the surface modified filler concentration (1, 3, 5 and 7 wt%) on the dielectric behaviour of the nano-hybrids was also studied. The thermodynamic parameters like activation energy (E_a), Arrhenius factor (A), entropy (ΔS), enthalpy (ΔH) and Gibbs free energy (ΔG) were calculated from TG-DTA results. The glass transition temperature was analyzed using differential scanning calorimetry (DSC).

2 Experimental

2.1 Infrared Spectra (ATR-FTIR)

The ATR-FTIR spectra were recorded on a Perkin Elmer 781 ATR-FTIR spectrometer that determines the chemical bonds of ZnO-APTES-DGEBA nanocomposite films. Vibration bands are reported as wave number (cm^{-1}).

2.2 Scanning Electron Microscopy (SEM)

A JEOL JSM-6360 Scanning electron microscope was used for sample analysis. The nanocomposite film was prepared by coating gold on the surface of the samples.

2.3 Atomic Force Microscopy (AFM)

The surface topology of the epoxy nanocomposite film was investigated by means of an AFM Seiko SPI3800N, series SPA-400 (Tokyo, Japan).

2.4 Thermal Analysis (TGA)

The thermal properties of the samples were studied by thermogravimetric analysis (TGA) (TA instrument-2000 Perkin Elmer) at a heating rate of 10 °C/min in an inert N_2 atmosphere.

2.5 Differential Scanning Calorimetry (DSC)

From DSC analysis, the glass transition temperature, the melting point and the crystallization/melting curve can be determined. The value of the entropy of fusion can be deduced and subsequently the percentage crystallinity in the sample can be calculated from this technique. DSC measurements were carried out with a PerkinElmer DSC 7 in the range of 30 to 200 °C in nitrogen atmosphere at a heating rate of 20 °C /min.

2.6 Dielectric Analysis

The dielectric properties of the neat and the ZnO-APTES modified systems were tested with the help of an impedance analyzer (Solartron impedance/gain phase analyzer 1260) at temperatures 30, 60 and 120 °C using platinum (Pt) electrodes at a frequency range of 1 MHz. This experiment was repeated four times at the same conditions.

$$\text{Dielectric Constant} = \text{Capacitance of dielectric/Capacitance of vacuum}$$

2.7 Materials and Methods

Epoxy resin GY250 a diglycidyl ether of bisphenol-A (DGEBA) with an epoxy equivalent weight (EEW) 182–192 (E.wt/g) and a viscosity of approximately 10,000 mPa was used for our study. Aradur HY951 curing agent was obtained from Huntsman (India). The red iron oxide pigment and 3-aminopropyltriethoxysilane (APTES) were purchased from Sigma Aldrich Chemicals. Acetone, O-xylene, NaOH were purchased from Sisco Research Laboratories, India.

2.8 Preparation of ZnO Nanoparticles

ZnO nanoparticles (NPs) were made according to the method of Singh et al. (2013) [11]. For the synthesis of ZnO, NaOH (0.4 M), and zinc acetate (0.2 M), solutions were mixed slowly with molar ratio of 2:1, respectively. The solution was stirred for 10 min. After that, 1.2 ml of triethanolamine (TEA) was added, and stirring continued for another 10 min. The solution was microwave irradiatied at 700 W in two steps, initially at 40 °C for 20 min later at 60 °C for 30 min. The resulting precipitate was washed 2-3 times with DI water. Furthermore, the sample was dried at 70 °C for 4 h using a hot air oven, then it was crushed using a mortar and pestle calcinated in air at 500 °C for 1 h.

2.9 Surface Treatment of ZnO Nanoparticles

The introduction of reactive NH_2 groups onto the surface of ZnO nanoparticles was achieved through the reaction between 3-aminopropyltriethoxysilane and hydroxyl groups on the ZnO nanoparticle surface. Typically, 2.0 g of ZnO NPs and 2 ml of 3-aminopropyltriethoxysilane were added in 40 ml O-xylene and the mixure kept at 150 °C for 3 h under ultrasonic bath stirring and argon protection. The reaction mixture was refluxed for 24 h. A rotary evaporator was used to remove the solvent from the 3-APTES modified ZnO. The ZnO nanoparticles were collected by filtration and rinsed three times with acetone. Afterwards, the 3-APTES functionalized ZnO nanoparticles were dried under vacuum for 12 h.

2.10 Preparation of ZnO-APTES-DGEBA Nanocomposite Films

The epoxy resin was prepared using a high speed disperser. The fabrication processes of ZnO-APTES-DGEBA nanocomposites were as follows. Different weight percentages of silane modified ZnO nanoparticles (0, 1, 3, 5 and 7 wt%) were directly added to a vessel charged with epoxy resin and solvent mixture (butanol/xylene) followed by addition of additives. The pigment was dispersed by stirring at 400 rotations per minute (rpm) for 30 min and then the stirrer speed was increased to 2000 rpm. The vessel was externally cooled using cold water to avoid a rise in temperature during processing. The dispersion was continued for 45-60 min to give a uniform red colored resin. For curing, the epoxy resin and curing agent (HY951) were mixed in a weight ratio of 100:58. The mixture was degassed in the vacuum oven for another 20 min at 40 °C to remove any gas bubbles generated during the mixing process. A mixture of solvents, xylene and butanol was used for dilution as convenient. The same method was repeated for different formulations of nanocomposite films and is listed in Table 1. The films were left for about 2 weeks at room temperature for complete curing. The reaction scheme of the ZnO-APTES-DGEBA nanocomposite is depicted in Scheme 1.

3 Results and Discussion

3.1 ATR-FTIR Analysis of ZnO-APTES-DGEBA Nanocomposite Films

Figure 1 shows the transmittance spectra for 1, 3, 5 and 7% ZnO-APTES-DGEBA nanocomposites in comparison with neat DGEBA resin. The major peaks were found in two spectral regions of 1800–600 cm^{-1} and

Table 1 Nomenclature of epoxy nanocomposites

Epoxy Resin	Pigment	Surface modified NPs Composition (Wt %)				Curing agent
		1%	3%	5%	7%	
DGEBA	×	×	×	×	×	HY951
	✓	ZnO-APTES	×	×	×	
	✓	×	ZnO-APTES	×	×	
	✓	×	×	ZnO-APTES	×	
	✓	×	×	×	ZnO-APTES	

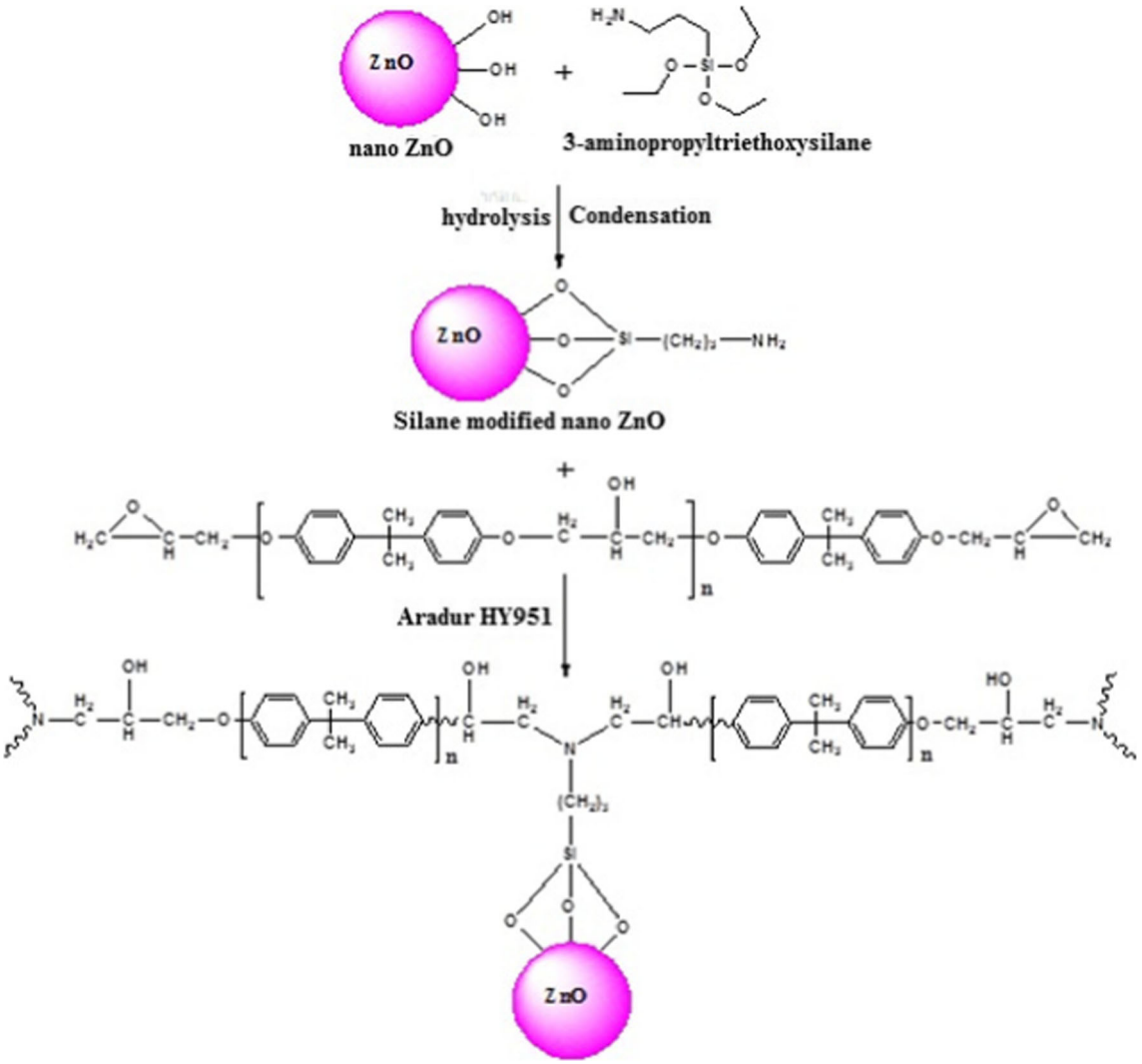

Scheme 1 Reaction route of ZnO-APTES-DGEBA nanocomposite

3500–2700 cm^{-1}. The tentative frequency assignments are tabulated in Table 2. The peak at ~ 1032 cm^{-1} of pure epoxy resin (DGEBA) assigned to asymmetrical aromatic C-O stretching is shifted to 1011, 1007, 997 and 987 cm^{-1} in 1, 3, 5 and 7% ZnO-APTES-DGEBA nanocomposites respectively. The ~1032 cm^{-1} peak explains the variation in etheric linkages of ZnO-APTES core shell nanoparticles with the epoxy resin. There is significant variation in transmitted intensities of all the peaks assigned in Table 2, which confirms the interation of ZnO-APTES-DGEBA nanocomposites with the epoxy resin. Usually a broad peak obtained between 3200–3450 cm^{-1} is assigned to –OH due to the interaction between the nanoparticle and epoxy resin whereas here the very weak band obtained in this region is due to the presence of functionalized ZnO nanoparticles [12, 13].

3.2 SEM Snalysis of ZnO-APTES-DGEBA Nanocomposite Films

From Fig. S1, it was found that the ZnO-APTES core shell nanoparticles are spherical in shape. The image shows that the ZnO-APTES core shell nanoparticles were homogeneously dispersed in the epoxy matrix. The unmodified ZnO nanoparticles were more aggregated when compared to functionalized nanoparticles in epoxy nanocomposites. The aggregation of nanoparticles might induce cracks in the nanocomposite films. Because there was no grafted epoxy resin on the ZnO surface, the compatibility between ZnO and epoxy resin was poor and interface bonding between nanoparticles and epoxy resin was weak. After functionalization, the compatibility and interface bonding between nanoparticles and epoxy resin were improved; the

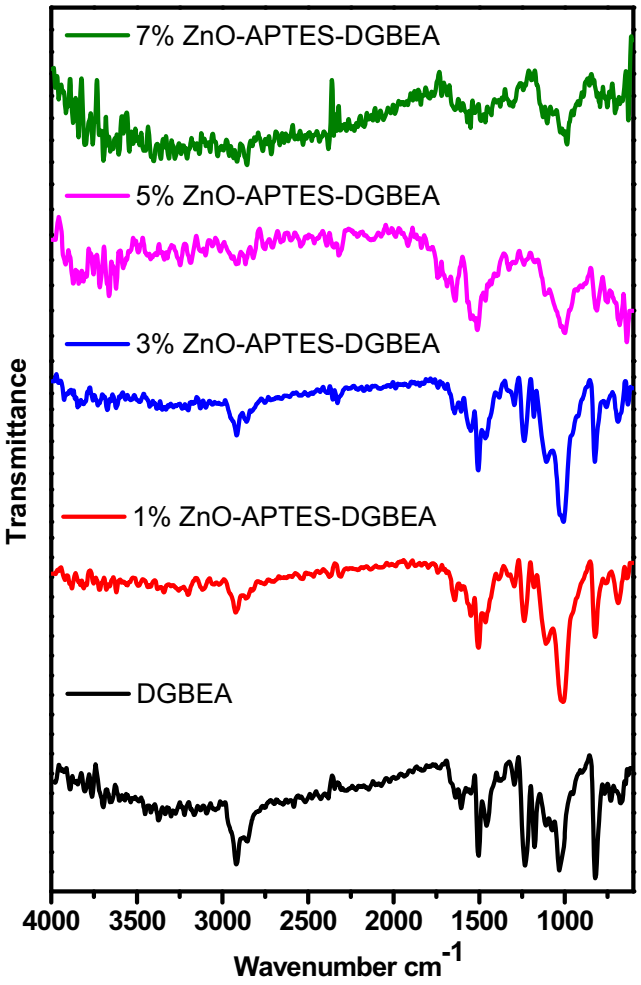

Fig. 1 ATR-FTIR spectra of DGBEA and ZnO-APTES-DGEBA nanocomposite films for spectral range (4000-600 cm^{-1})

aggregation of ZnO-APTES and the cracks around the aggregation decreased. For epoxy nanocomposite films containing unmodified ZnO nanoparticles, relatively large particle aggregates with a non-uniform distribution appeared on the surface of the samples [14]. However, with ZnO-APTES core shell nanoparticles, the aggregation on the surface of the film was less and a more uniform distribution of nanoparticles appeared on the surface of the epoxy nanocomposite film.

3.3 AFM Analysis of ZnO-APTES-DGEBA Nanocomposite Films

Figure S2 shows the AFM 3D and topographic image of the best system under study 3%-ZnO-APTES-DGEBA nanocomposite film. AFM analysis is used to obtain the distribution of ZnO nanoparticles in the epoxy resin. The morphology with smooth and fused surfaces and weak accumulation of particles was clearly resolved from the AFM images. Most of the particles are homogeneously distributed due to surface functionalization of ZnO nanoparticles. These results almost agree with the SEM results thereby adding evidence for the surface morphology.

3.4 TG-DTA Studies

The TGA curve shows two decomposition stages exist in all the samples shown in Fig. 2. In neat epoxy resin the first decomposition stage starts at 325 °C and the second stage at 513.2 °C. The temperature of the first decomposition stage for 1 and 3%-ZnO-APTES-DGEBA increases compared to the neat epoxy resin whereas it decreases at higher concentrations of 5 and 7%-ZnO-APTES-DGEBA nanocomposite film. The temperature of the second stage decomposition increases in all the samples compared to the neat epoxy resin. The melting point temperature is obtained from the DTA curve, given in Fig. 3. The melting point temperature decreases in all the samples except 5%-ZnO-APTES-DGEBA compared to the neat epoxy resin. The variation in decomposition temperature and in melting point temperature might be due to the surface interaction of the nanoparticle and epoxy layer [15, 16].

3.4.1 Kinetic Analysis

The kinetic parameters were calculated using the Coats-Redfern method as tabulated in Table 3. The kinetic parameters were calculated for the main stage of decomposition in all the epoxy nanocomposites. The decomposition stages, melting point and the calculated thermodynamic parameters are given in Table 4. The activation energy E_a decreases for samples 1, 5 and 7%-ZnO-APTES-DGEBA but increases in the 3%-ZnO-APTES-DGEBA sample. This implies the thermal stability is high for a particular optimum filler concentration, at low filler concentration it is not adequate and at higher concentration the agglomeration of nanoparticles will affect the thermal stability of the epoxy nanocomposites. The positive values of the Gibbs free energy (ΔG) of all the epoxy nanocomposite films shows the decomposition is non-spontaneous and has to be initiated by an external source. The calculated enthalpy values are positive for all the samples which explains the process is endothermic in nature and enhances with rise in temperature. The calculated entropy values are found to be negative which indicates the activated complex is more ordered than the reactor, also the reaction is slow in nature. However the frequency factor in the Arrhenius equation is very high which accelerates the process to a faster rate. From the calculated kinetic parameters, the

Table 2 Tentative frequency assignment of 1, 3, 5 and 7% ZnO-APTES-DGEBA nanocomposite films

DGBEA	1% ZnO-APTES-DGBEA	3% ZnO-APTES-DGBEA	5% ZnO-APTES-DGBEA	7% ZnO-APTES-DGBEA	Tentative frequency assignment
Wavenumber (cm^{-1})					
630 (vw)	638 (vw)	632 (w)	638 (w)	628 (w)	C-O-O bonding (aromatics)
673 (vw)	687 (w)	689 (w)	677 (w)	677 (vw)	CH_2 bending vibration
822 (m)	822 (s)	824 (s)	814 (w)	811 (vw)	–CH out of plane deformation in aromatic
1032 (m)	1011 (vs)	1007 (vs)	997 (m)	987 (m)	asymmetrical aromatic C-O stretch
1109 (vw)	1109 (s)	1107 (s)	1115 (vw)	1103 (vw)	asymmetrical aliphatic C-O stretch
1177 (m)	1179 (w)	1181 (m)	1173 (vw)	–	–CN vibration
1232 (m)	1238 (m)	1236 (s)	1238 (w)	1242 (w)	asymmetrical aromatic C-O stretch
1295 (w)	1295 (m)	1295 (m)	1289 (vw)	1291 (vw)	asymmetrical-CH_2 deformation
1456 (m)	1462 (s)	1464 (s)	1462 (w)	1464 (w)	C-C stretching vibration in aromatic
1503 (s)	1503 (vs)	1505 (vs)	1509 (w)	–	
1548 (vw)	1548 (m)	1548 (m)	1550 (vw)	1550 (vw)	
1638 (w)	1642 (m)	1642 (m)	1642 (m)	1644 (w)	
2854 (m)	2862 (w)	2858 (m)	2864 (vw)	2856 (m)	CH_2 symmetric stretching
2917 (m)	2923 (m)	2915 (s)	2919 (vw)	2915 (w)	asymmetrical C-H stretch of –CH2 group
3417 (vw)	3419 (vw)	3425 (vw)	3419 (vw)	3417 (w)	

w-weak band, vw-very weak band, m-medium, s-strong, vs-very strong

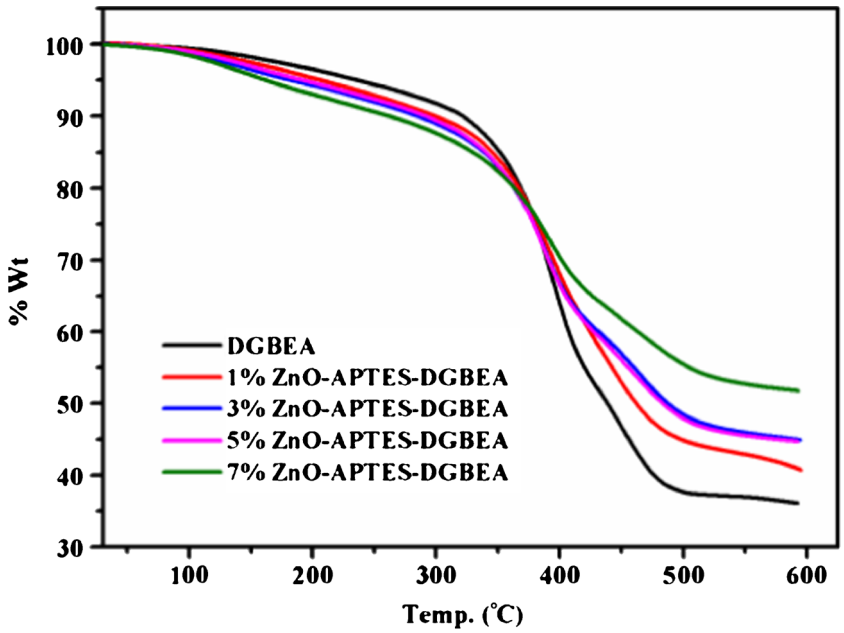

Fig. 2 TGA curve for ZnO-APTES-DGEBA nanocomposite films

3%-ZnO-APTES-DGEBA nanocomposite film is the optimum concentration in this study which exhibits excellent thermal properties compared to the other epoxy nanocomposites.

3.5 Analysis of Glass Transition Temperature (T_g) Using DSC

The glass transition temperatures (T_g) of DGEBA, 1, 3, 5 and 7% ZnO-APTES-DGEBA nanocomposite films are shown in Fig. 4. The glass transition temperature (T_g) of DGEBA is 105.4 °C which closely matches with the standard values of epoxy resin. The T_g values of all epoxy nanocomposites vary differently with filler concentration. The T_g values of 1, 3 and 7% ZnO-APTES-DGEBA epoxy nanocomposite films are 88.2 °C, 102.6 °C and 87.8 °C respectively which is less than the T_g value of DGEBA sample whereas the 5% ZnO-APTES-DGEBA film exhibits a slight increase in T_g value with 107.7 °C. A similar observation of a reduction in the values of T_g with addition of small amounts of nano-fillers has been reported for alumina filled PMMA nanocomposites [17]. T_g can reduce in polymer composites due to various reasons like changes in molecular

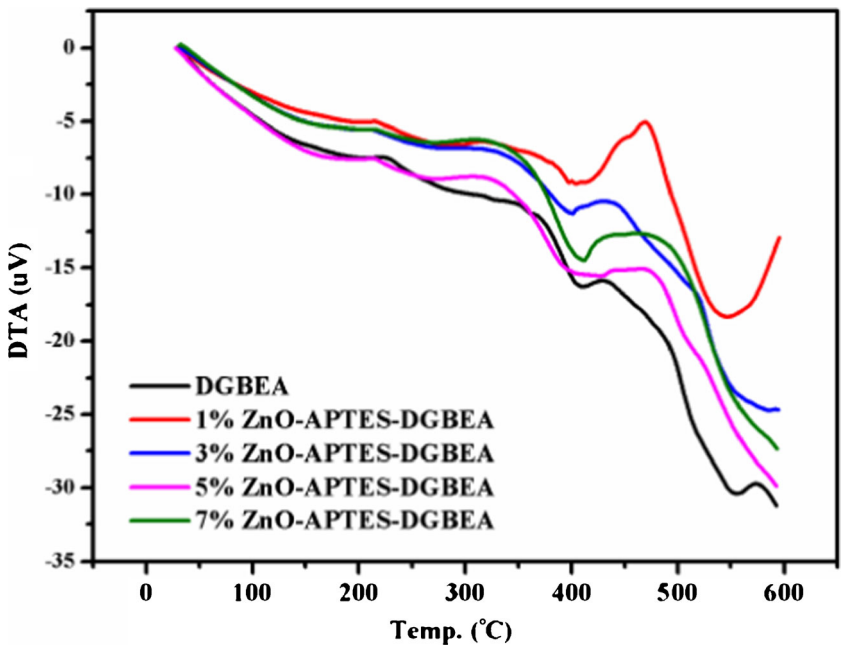

Fig. 3 DTA curve for ZnO-APTES-DGEBA nanocomposite films

Table 3 Formulas used to calculate the thermodynamic parameters from TGA results

Thermodynamic parameters	Formula
Activation energy (E_a)	$-E = \left[\frac{slopex2.303xR}{1000}\right] kj/mol$
Frequency factor in Arrhenius equation (A)	$\left[\frac{AR}{\alpha E}\right]\left[1-\frac{2RT}{E}\right]-\left[\frac{E}{2.303RT}\right] = e^{intercept}$
Enthalpy (ΔH)	$\Delta H = E - 2RT kj/mol$
Entropy (ΔS)	$\Delta S = 2.303R\log\left(\frac{Ah}{kT_m}\right) kj/mol$
Gibbs free energy (ΔG)	$\Delta G = \Delta H - T\Delta S\ kj/mol$

weight, tacticity and cross-linking density. But, in the present investigations, the processing method used to prepare the epoxy nanocomposites is the same for the different filler concentrations. Therefore, it is expected that the variations in the glass transition temperatures are influenced by the interaction of nanoparticles and the epoxy. Further, it has also been recently reported that there is a significant influence of humidity on the T_g of nanocomposites and the presence of a water nanolayer on the surface of the nanoparticles can lead to a reduction in the T_g values. The occurrence of a water nanolayer in the present experiments is very unlikely since the particles are thoroughly dried before they are dispersed in epoxy and also the nanocomposite sample preparations are carried out under tight ambient control to ensure that there is no influence of humidity. Reports suggest that interactions between polymer chains and the highly charged nanoparticle surface lead to the formation of a polymer nanolayer close to the nanoparticle surface and it is this interfacial nanolayer which determines the glass transition temperatures (T_g). These nanoparticle-polymer interactions can be attractive, repulsive or neutral and depending on these behaviors, T_g can increase, decrease or remain constant. It is suggested that polymer-nanoparticle interactions actually lead to the formation of two nanolayers around the nanoparticle [18, 19]. The first nanolayer closest to the nanoparticle surface is assumed to be tightly bound to the surface resulting in the polymer chains there being highly immobile. Then there is a formation of a second polymer nanolayer with a thickness slightly more than that of the first layer and this layer contains polymer chains which are loosely bound. It seems that this loosely bound polymer in the extended layer causes a reduction in the nanocomposite glass transition temperatures at low nano-filler concentrations. For the present nanocomposite system with ZnO fillers, it is difficult to predict the interaction process (attractive, repulsive or neutral) from the measured T_g results. Since T_g in the nanocomposites is observed to reduce with all filler loadings except 5% filler concentration in the present study, the system is expected to be a repulsive one wherein the

Table 4 Thermodynamic parameters calculated from TGA results

SAMPLE	Decomposition		Melting point °C	E_a kj/mol	A $\times 10^5$ kj/mol	ΔH $\times 10^4$ kj/mol	ΔS kj/mol	ΔG $\times 10^5$ kj/mol
	1st stage °C	2st stage °C						
DGBEA	325	513.2	411.8	18.79	1.48	0.88	−145.97	0.96
1%- ZnO-APTES-DGBEA	330	517.7	407.3	17.26	1.53	0.72	−145.79	0.95
3%- ZnO-APTES-DGBEA	333	541.7	398.1	26.20	0.44	1.61	−156.17	1.11
5%- ZnO-APTES-DGBEA	322	556.4	417.5	23.25	0.64	1.34	−152.92	1.04
7%- ZnO-APTES-DGBEA	313	559.9	410.3	20.22	0.70	1.05	−152.07	1.00

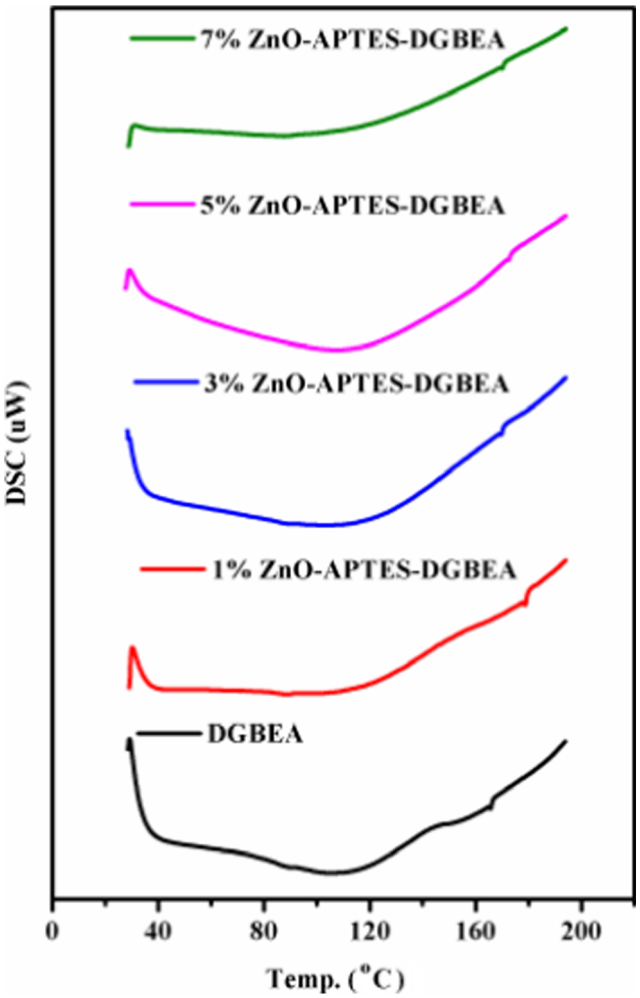

Fig. 4 DSC curve for ZnO-APTES-DGEBA nanocomposite films

polymer chains in the interfacial nanolayer relax faster. At lower nano-filler concentrations, the filler distributions in the polymer are usually uniform with large inter-particle distances and hence the interfacial effects in nanocomposites may be much more pronounced.

3.6 Dielectric Studies of ZnO-APTES-DGEBA Nanocomposite Films

The dielectric spectroscopy results of neat epoxy resin DGEBA, 1, 3, 5 and 7% ZnO-APTES-DGEBA nanocomposite films are shown in Figs. 5, 6 and 7. The dielectric measurements were carried out at three different temperatures 30 °C, 60 °C and 120 °C and are shown as (a), (b) and (c) respectively in all images from Figs. 5–7.

3.6.1 Frequency Dependence

The frequency dependence of dielectric permittivity illustrated in Fig. 5a–c, which shows the real part of the permittivity (ε_r') decreases with increase in frequency for DGEBA epoxy resin and for all tested epoxy nanocomposites 1, 3, 5 and 7% ZnO-APTES-DGEBA epoxy nanocomposite films. This dependence is observed for all the filler concentrations and at various temperatures studied. In epoxy nanocomposite films the slope of the permittivity decrease is higher at lower frequencies (up to 10–100 Hz) than at higher frequencies, indicating a "low frequency dispersion" (LFD) or "quasi-DC" (QDC) behavior [20]. This behavior of epoxy nanocomposites is thought to be due to a transition from an intercluster to an intracluster charge movement combined with a transition from large scale to small scale molecular motions inside the polymers when passing from lower to higher frequencies. Thus, the Dissado and Hill model to explain LFD is based on the concept of clusters, which is a region with partial structural regularity in which there are quasi-mobile ions moving by hopping to unoccupied sites. If the access to sites is restricted then conduction may be due to a combination of intracluster and intercluster motions. The decrease of ε_r' with the frequency at mid-range frequencies (above 100 Hz) was mainly ascribed to the reduction of the polarizations caused by dipolar groups both in the neat polymer and in nanoparticles [21, 22]. Thus, in a typical epoxy system (epoxy resin cured with an amine hardener) as in the present case, the dipoles of the molecular groups which are transversally attached to the longitudinal polymer chain are easier to orient by the electric field at low frequencies resulting in a high permittivity. These free dipolar groups become more difficult to orient by the electric field at higher frequencies, so their contributions to the effective permittivity decrease with the frequency. On the other hand, the ionic relaxation and dipolar relaxation mechanisms play important roles in deciding the dielectric permittivity of the epoxy system under study. It is well known that the interfacial or space charge polarization tends to occur at the interfaces. Since epoxy/nanocomposites have a large volume fraction of interfaces therefore the interfacial polarization is expected to play an important role [23, 24]. The interfacial polarization occurs when charge carriers are trapped at the interfaces of these heterogeneous systems. As the frequency of the applied electric field increases, it is more difficult for space charges to be trapped at the interfaces which reduces the interfacial polarization thereby decreasing dielectric permittivity as the frequency increases. This explains why the relative permittivity decreases as the frequency increases.

Figure 6a-c shows the dielectric loss at 30, 60, 120 °C for DGEBA and epoxy nanocomposite films. The dielectric loss in DGEBA, 3 and 5% ZnO-APTES-DGEBA epoxy nanocompostie films exist at a low frequency region around 10–100Hz, but in the 1% ZnO-APTES-DGEBA sample the dielectric loss occurs up to a frequency region around 10^3 – 10^4 Hz at 30 and 60 °C; however, it occurs beyond 10^4 Hz at

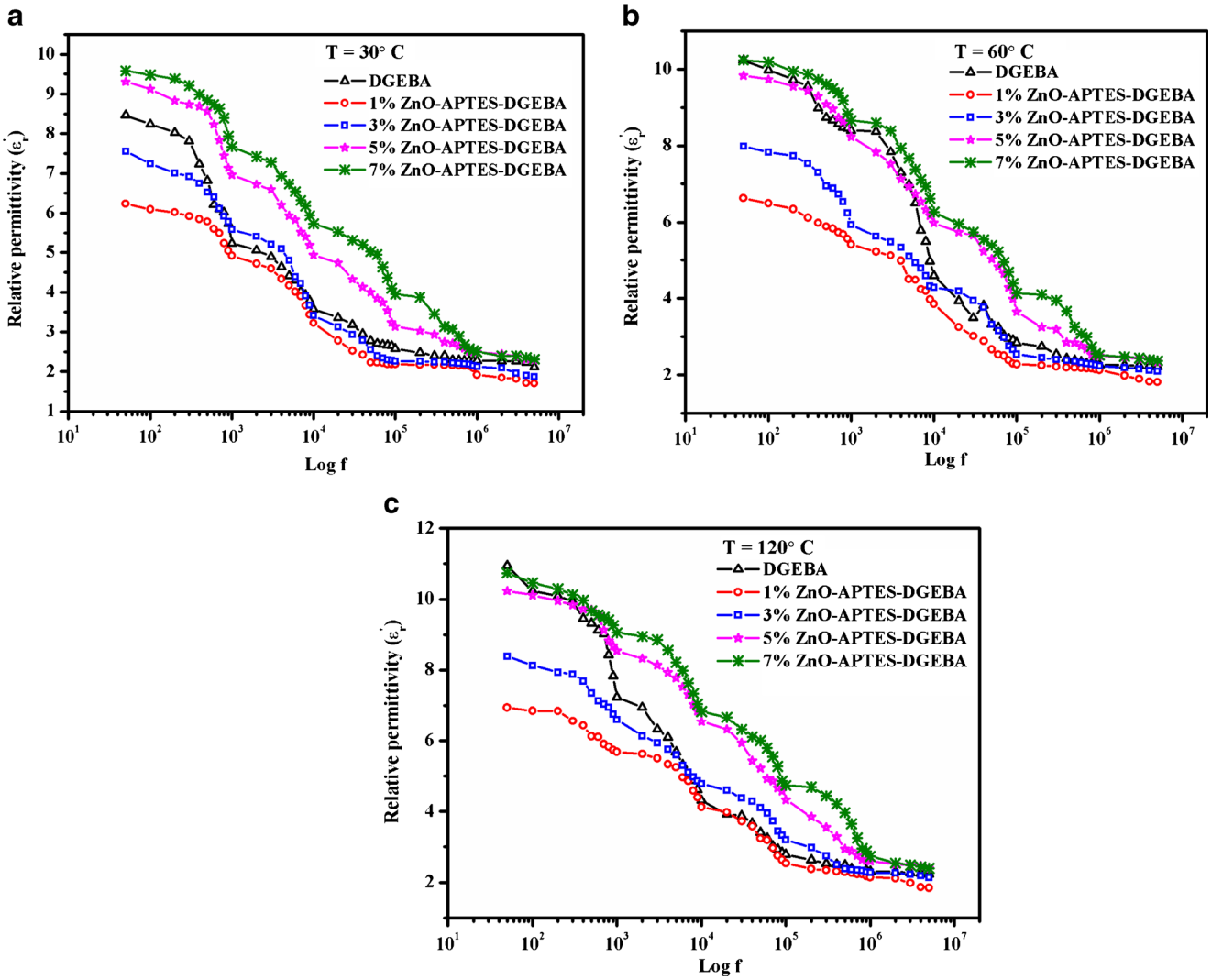

Fig. 5 Relative permittivity plots for ZnO-APTES-DGEBA nanocomposite films **a** 40 °C **b** 80 °C **c** 120 °C

120 °C. The dielectric loss occurs up to the frequency range of 10^2–10^3 Hz in the 7% ZnO-APTES-DGEBA sample at 60 and 120 °C compared to the DGEBA sample.

The dielectric loss or tan δ value is used to describe the ability of the dielectric materials to dissipate heat energy. The tan δ value in the low frequency range (below 10Hz) is believed to be due to both ionic relaxation and dipole relaxation phenomena. Further increase in the tan δ value at the higher frequency range (above 100Hz) is believed to be due to the increase in relaxation loss of epoxy resin polar groups under a high frequency field. The ionic polarization could also occur in a higher frequency range and leads to further increase in the tan δ value. Under an alternating electric field, the tan δ value of polymer materials depends on not only frequency, but also on the conductivity and the relaxation time of large molecular chains. The dielectric loss of polymer materials could be due to both conductivity loss which is caused when the charge carriers travel across the materials under the applied field and orientation polarization of large molecules under the applied field. As the resistivity of an epoxy is around 10^{13}–10^{14} Ωm, the conductivity loss of the epoxy is small. Moreover, the epoxy resin tends to form a large 3D cross-linking network during curing. Such a 3D network structure restricts the orientation polarization of large molecule. So the relaxation loss caused by polar groups is the main factor in determining the dielectric loss of epoxy resins as the orientation polarization is mainly caused by the direction of polar groups [25].

The epoxy nanocomposites do not exhibit electrical conductivity at the low frequency region. However the AC conductivity of all the samples increases at the high frequency range of 10^6–10^7 Hz. This might be due to the increase in diffusion of ions through the epoxy nanocomposites at higher frequencies or due to the change in dielectric loss with frequency as described above.

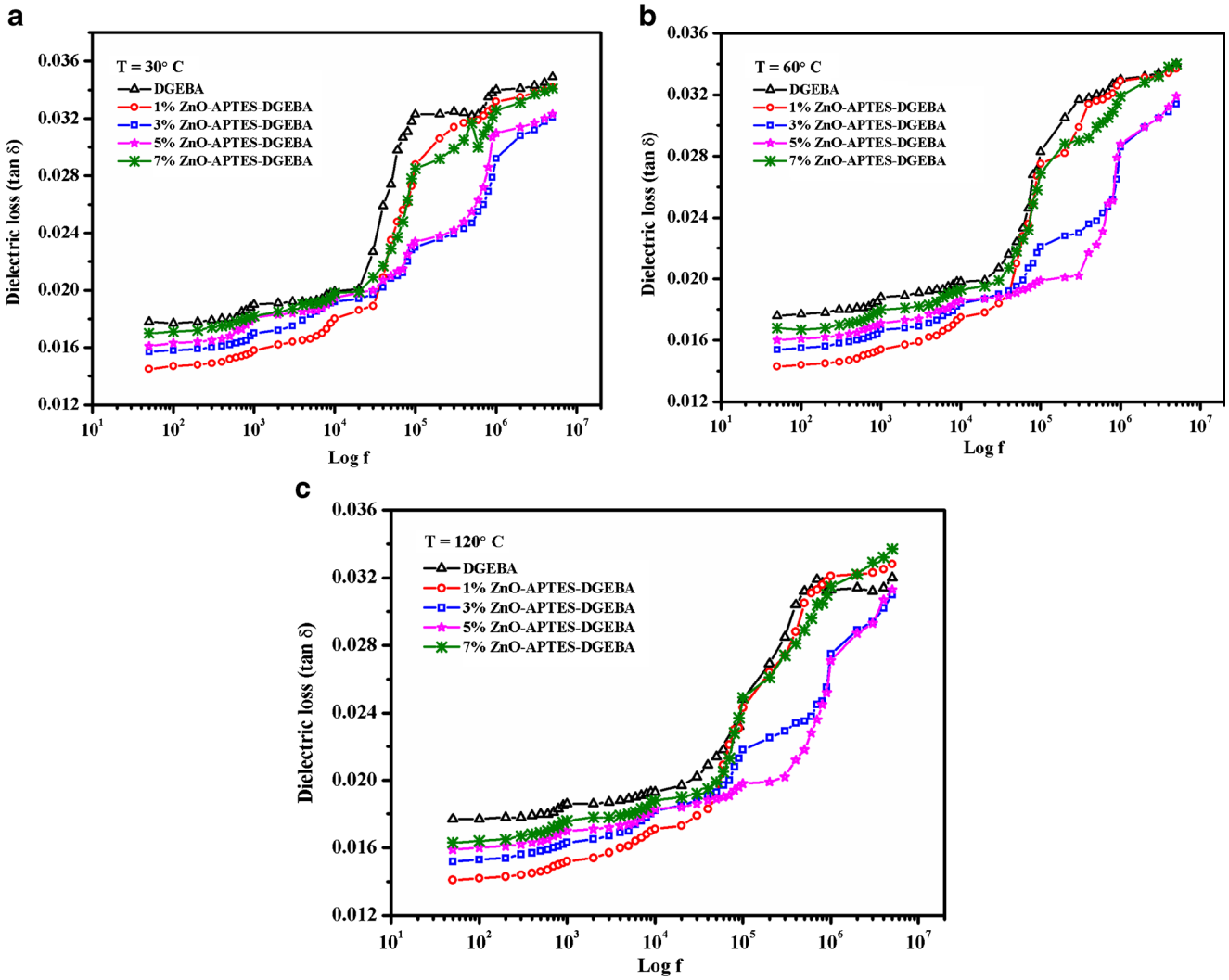

Fig. 6 Dielectric loss plots for ZnO-APTES-DGEBA nanocomposite films **a** 40 °C **b** 80 °C **c** 120 °C

3.6.2 Temperature Influence

The real part of the permittivity ε_r' of DGEBA and epoxy nanocomposites samples increases with increase in temperature, attributed to the increase in molecular dipole moment as temperature increases. The increased segmental mobility of the polymer facilitates the orientation of dipoles, thereby leading to an increase in dielectric constant. The frequency variation of the dielectric loss at various temperatures shows that it is high at 30 °C and it decreases as the temperature increases to higher values. The dielectric loss of polymer materials could be due to both conductivity loss and orientation polarization of large molecules under an applied field. As the temperature increases the conductivity loss decreases and the orientation of larger molecules is affected which contributes to the decrease in dielectric losses. The temperature variation of AC conductivity is shown in Fig. 7a–c. As the temperature increases the AC conductivity of DGEBA and epoxy nanocomposites samples decreases but increases at higher loading concentration of 5 and 7% APTES-ZnO where the ionic polarization of filler nanoparticles is dominant. This is evident from the decrease in orientation polarization of molecular groups with increase in temperature and the temperature independent behavior of ionic polarization in filler nanoparticles [26].

3.6.3 Effect of Concentration

The real part of the permittivity ε_r' of 1 and 3% ZnO-APTES-DGEBA samples is low compared to the DGEBA epoxy sample, especially at lower frequencies and at various temperatures measured. When a small amount of nanofiller is loaded into an epoxy, due to the interaction between filler and epoxy chain, the thin immobile nanolayers can be formed. These thin immobile nanolayers will restrict the mobility of the epoxy chain [27]. As the loading

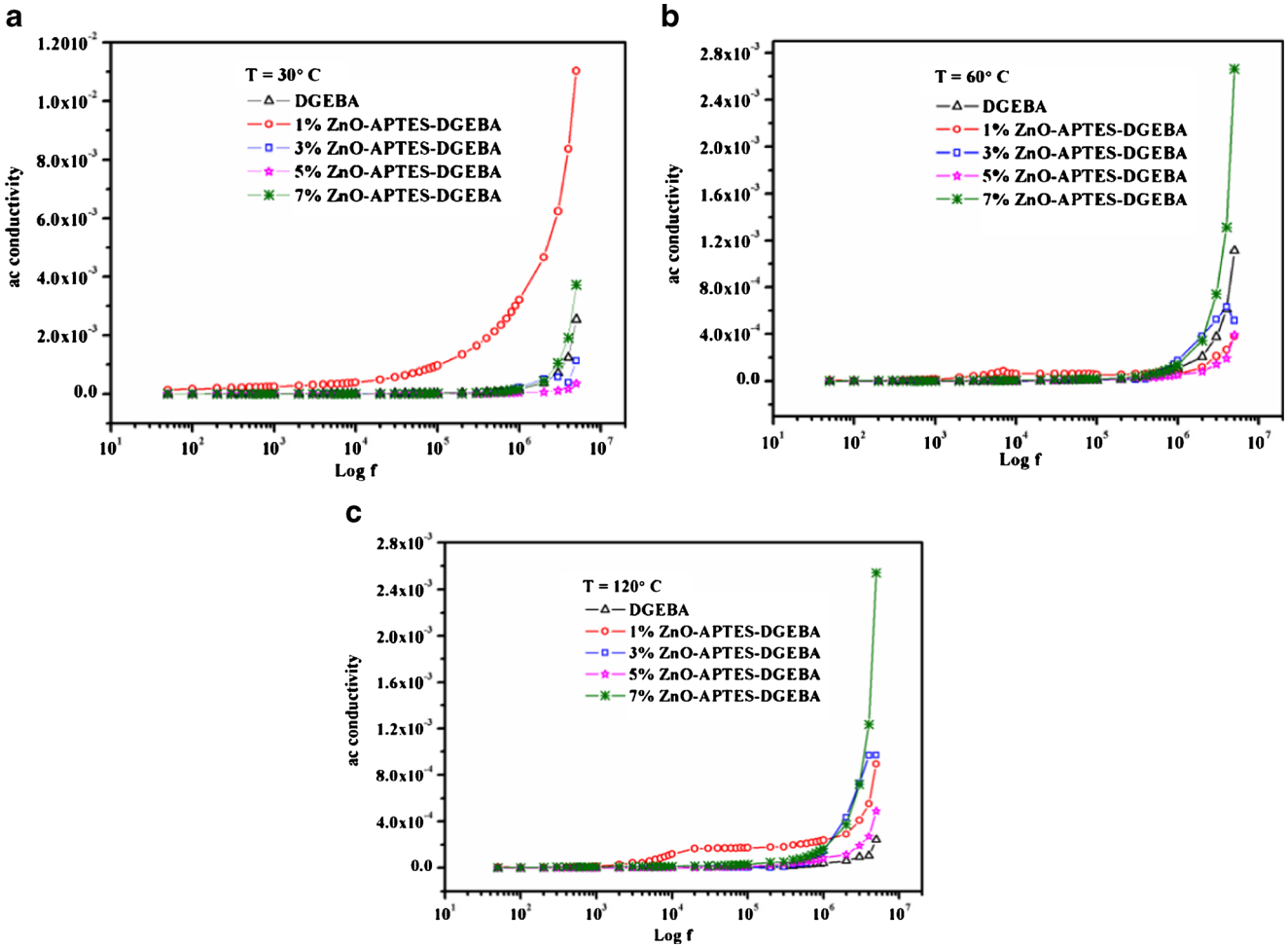

Fig. 7 AC conductivity plots for ZnO-APTES-DGEBA nanocomposite films **a** 40 °C **b** 80 °C **c** 120 °C

concentration increased to 5 and 7% APTES-ZnO, the effective permittivity of the epoxy nanocomposite film increases. It is known that the nanosize APTES-ZnO fillers have higher permittivity compared to the neat epoxy resin. That could be one of the reasons leading to an increase of effective permittivity with higher loading concentrations. The dielectric loss is low in 1 and 3% ZnO-APTES-DGEBA nanocomposite films compared to neat epoxy, 5 and 7% nanocomposite films. As the filler concentration increases the molecular dipole moment decreases which influences the decrease in dielectric losses at higher concentration. The AC conductivity of epoxy nanocomposties increases with increase in filler loading concentration. Initially at 30 °C the conductivity is high in the 1% ZnO-APTES-DGEBA nanocomposite film compared to the other sample since higher concentration of fillers will affect the mobility of charge carriers. Contrastingly at 60 and 120 °C temperatures, the AC conductivity of the 7% ZnO-APTES-DGEBA nanocomposite film is higher compared to all other samples. The main reason is the increase in mobility of charge carriers at elevated temperatures.

4 Conclusions

The synthesized epoxy nanocomposite matrices with various filler concentration of ZnO-APTES core shell nanoparticles were structurally confirmed with ATR-FTIR, SEM and AFM studies and it was also found that ZnO-APTES is uniformly dispersed in epoxy matrices. From TG-DTA studies the melting point and the decomposition stages are found to vary with filler concentration in all epoxy nanocomposites compared to the control samples. Also the calculated kinetic parameters suggest the 3% ZnO-APTES-DGEBA sample is the optimum system having excellent thermal properties compared to the other epoxy nanocomposites. The glass transition temperature T_g in the nanocomposites is observed to reduce with all filler loadings except 5% filler concentration. In the present study, the system is expected to be a repulsive one wherein the polymer chains in the interfacial nanolayer relax faster. The real part of permittivity, dielectric loss and AC conductivity show significant changes with filler concentration, temperature and frequency. The dielectric

behavior improves by adding ZnO-APTES as nanosized fillers in the epoxy resin.

References

1. Karunakaran C, Jayabharathi J, Jayamoorthy K (2013) Benzimidazole: Dramatic luminescence turn-on by ZnO nanocrystals. Measurement 46:3883–3886
2. Li J, Li L, Xiang Y, Zheng S (2016) Nanostructured Epoxy Thermosets Containing Poly(vinylidene fluoride): Preparation, Morphologies, and Dielectric Properties. Ind Eng Chem Res 55:586–596
3. Jlassi K, Chandran S, Poothanari MA, Zayani MB, Thomas S, Chehimi MM Clay/polyaniline hybrid through diazonium chemistry: conductive nanofiller with unusual effects on interfacial properties of epoxy nanocomposites. Langmuir. https://doi.org/10.1021/acs.langmuir.5b04457
4. Xiong J, Liu Y, Yang X, Wang X (2004) Thermal and mechanical properties of polyurethane/montmorillonite nanocomposites based on a novel reactive modifier. Polym Degr Stab 86:549–555
5. Duraibabu D, Alagar M, Ananda Kumar S (2014) Studies on mechanical, thermal and dynamic mechanical properties of functionalized nanoalumina reinforced sulphone ether linked tetraglycidyl epoxy nanocomposites. RSC Adv 4:40132–40140
6. Kornmann X, Thomann R, Mulhaupt R, Finter J, Berglund LA (2002) High performance epoxy-layered silicate nanocomposites. Polym Eng Sci 42:1815–1826
7. Kinloch AJ, Shaw SJ, Hunston DL (1983) Microstructure and fracture studies. Polymer 32:1341–1354
8. Meenakshi KS, Jaya Sudhan EP (2011) Development and study of the thermal and electrical behaviour of TGDDS epoxy nanocomposites for high-performance applications. Appl Nanosci 1:109–115
9. Clayton A (1988) Epoxy resins: chemistry and technology. Marcel Decker, New York
10. Guenthner AJ, Yandek GR, Wright ME, Petteys BJ, Quintana R, Connor D, Gilardi RD, Marchant D (2006) A new silicon-containing Bis(cyanate) ester resin with improved thermal oxidation and moisture resistance. Macromolecules 39:6046–6053
11. Saravanan P, Jayamoorthy K, Ananda Kumar S (2015) Switch-On fluorescence and photo-induced electron transfer of 3-aminopropyltriethoxysilane to ZnO: Dual applications in sensors and antibacterial activity. Sensors Actuators B: Chem 221:784–791
12. Nikolic G, Zlatkovic S, Cakic M, Cakic S, Lacnjevac C, Rajic Z (2010) Fast fourier transform IR characterization of epoxy GY systems crosslinked with aliphatic and cycloaliphatic EH polyamine adducts. Sensors. https://doi.org/10.3390/s100100684
13. Suresh S, Saravanan P, Jayamoorthy K, Ananda Kumar S, Karthikeyan S (2016) Development of silane grafted ZnO core shell nanoparticles loaded diglycidyl epoxy nanocomposites film for antimicrobial applications. Mater Sci Eng C 64:286–292
14. Olad A, Nosrati R (2012) Preparation, Characterization, and photocatalytic activity of polyaniline/ZnO nanocomposite. Res Chem Intermed 38:323–336
15. Sharma P, Choudhary V, Narula AK (2008) Curing and thermal behavior of epoxy resin in the presence of a mixture of imideamines. J Therm Anal Calorim 94:805–815
16. Leszczynska A, Pielichowski K (2008) Application of thermal analysis methods for characterization of polymer/montmorillonite nanocomposites. J Therm Anal Calorim 933:677–687
17. Liška M, Antalík J (2004) Enthalpy relaxation in glasses: regression analysis of integral DSC data. J Therm Anal Calorim 67:213–222
18. Starr W, Schrøder T, Glotzer S (2001) Effects of a nanoscopic filler on the structure and dynamics of a simulated polymer melt and the relationship to ultrathin films. Phys Rev E 64:1802–1805
19. Ash B, Schadle L, Siegel R (2002) Glass transition behavior of Alumina/polymethyl methacrylate nanocomposites. Mater Lett 55:83–87
20. Nelson JK, Fothergill JC (2004) Internal charge behaviour of nanocomposites. Nanotechnology 15:586–595
21. Sasidhar S, Schuman TP, Dogan F (2013) Dielectric Properties of polymer−particle nanocomposites influenced by electronic nature of filler surfaces. ACS Appl Mater Interfaces 5:1917–1927
22. Lewis TJ (2006) Nano-composite dielectrics: The dielectric nature of the nano-particle environment. IEEJ Trans Fundam Mater 126:1020–1030
23. Plesa I, Ciuprina F, Notingher PV (2010) Dielectric spectroscopy of epoxy resin with and without inorganic nanofillers. J Adv Res Phys 1:011011
24. Huang X, Zheng Y, Jiang P, Yin Y (2010) Influence of nanoparticle surface treatment on the electrical properties of cycloaliphatic epoxy nanocomposites. IEEE Trans Dielectr Electr Insul 17:635–643
25. Roy M, Nelson JK, MacCrone RK, Schandler LS, Reed CW, Keefe R, Zenger W (2005) Polymer nanocomposites dielectrics – the role of the interface. IEEE Trans Diel and Electr Insul 12:629–643
26. Tanaka T, Montanari GC, Mülhaupt R (2004) Polymer nanocomposites as dielectrics and electrical insulation-perspectives for processing technologies, material characterization and future applications. IEEE Trans Diel and Electr Insul 11:763–784
27. Singha S, Thomas MJ (2008) Dielectric properties of epoxy nanocomposites. IEEE Trans Dielectr Electr Insul 15:12–23